The effect of the precursor structure on the catalytic properties of the nickel—chromium catalysts of hydrogenation reactions

I. I. Simentsova, T. P. Minyukova, A. A. Khassin, E. V. Dokuchits, L. P. Davydova, I. Yu. Molina, L. M. Plyasova, G. N. Kustova, and T. M. Yurieva*

G. K. Boreskov Institute of Catalysis, Siberian Branch of the Russian Academy of Sciences, 5 prosp. Akad. Lavrent´eva, 630090 Novosibirsk, Russian Federation. Fax: +7 (383) 330 8056. E-mail: sii@catalysis.ru

The influence of the Ni^{2+}/Cr^{3+} ratio in the precursor compound on the formation of the catalyst structure and its transformation upon the thermal treatment and reductive activation in hydrogen was studied. The precursors with the cation ratio Ni^{2+}/Cr^{3+} = (2.3—3)/1 represent a homogeneous system of the stichtite-type structure. The treatment of the precursors at T ~400 °C in an inert atmosphere forms a nanosized phase of the NiO-type structure with the lattice parameter a = 4.186±0.005 Å. At 600 °C the lattice parameter of this phase decreases to the tabulated value (a = 4.177±0.005 Å). The phase of nickel chromite of the cubic spinel structure with the lattice parameter a = 8.320±0.005 Å is also observed. Hydrogen activation of the catalyst preheated at 300 °C in an inert gas leads to the formation of Ni^0 crystallites with a size of ~5.5 nm and a specific surface area of ~7.0 $m^2\ g^{-1}$. This catalyst exhibits high activity and selectivity in benzene hydrogenation and preferential CO hydrogenation in the presence of CO_2. The catalysts with the ratio Ni^{2+}/Cr^{3+} = 1/(2—3) containing nickel and chromium hydroxocarbonates as precursors are less active in the hydrogenation of benzene to cyclohexane.

Key words: nickel—chromium catalysts, precursor compound, hydrogenation of benzene, preferential methanation of carbon monoxide.

Nickel-containing catalysts are widely used in the hydrogenation of unsaturated and aromatic hydrocarbons.[1—4] The catalysts manifest the hydrogenating activity after treatment in hydrogen, during which the nickel compounds are reduced to the metal. The catalyst activity depends on the size of the nickel particles on the catalyst surface. The studies[5—10] of the supported and coprecipitated nickel-containing catalysts in benzene hydrogenation showed that the samples with the crystallite size of Ni between 1 and 10 nm formed upon the reduction of the oxide precursors at 300—400 °C are most active. However, the influence of the structure of the nickel-containing oxide phase of the precursor on the formation of Ni^0 crystallites on the catalyst surface remains unclear.

In the present work, we studied the effect of the structural characteristics of the nickel—chromium oxide precursors on the properties of nickel crystallites formed during hydrogen activation.

Experimental

Precursor compounds of the nickel—chromium catalysts were prepared by the continuous coprecipitation of Ni^{2+} and Cr^{3+} from an aqueous solution of their nitrates at 65—70 °C and pH = 7.2—7.4. Sodium or ammonium carbonate was used as a precipitating agent. The precipitate was thoroughly washed with distilled water and dried under an IR lamp at T ~45 °C. The cationic composition of the obtained samples was determined by atomic emission spectroscopy (AES). The sodium content did not exceed 0.5 wt.%. The contents of nickel and chromium in the synthesized samples are given below. In the synthesis of the sample NiCr-3/1 ammonium carbonate was used as a precipitating agent, and sodium carbonate was used in other syntheses.

Code of sample	Relative atomic content of cations
NiCr-1/3	$Ni_{0.23}Cr_{0.77}$
NiCr-1/2	$Ni_{0.33}Cr_{0.67}$
NiCr-2.3/1	$Ni_{0.67}Cr_{0.33}$
NiCr-3/1	$Ni_{0.73}Cr_{0.27}$
Cr	$Cr(OH)_x(CO_3)_y$
Ni	$Ni(OH)_x(CO_3)_y$

Samples of nickel and chromium hydroxocarbonates used as reference samples were prepared under the same conditions as nickel—chromium hydroxocarbonates.

X-ray diffraction studies were carried out on a D-500 diffractometer (Siemens, Germany) in monochromatized Cu-Kα radiation (reflected-beam graphite monochromator). Diffraction patterns were detected using scanning by points in the 2θ range 5—70° with an increment of 0.05° and an accumulation time of 5 s in each point. The phase composition of the samples was identified using the ICDD-PDF2 and JCPDS international dif-

Published in Russian in *Izvestiya Akademii Nauk. Seriya Khimicheskaya,* No. 11, pp. 2002—2007, November, 2010.

fraction data bases. The determination error of the lattice parameters for well crystallized samples did not exceed ±0.005 Å.

The dimension of coherent scattering regions (CSR) was calculated from the integral half-width of diffraction lines. The international standard SRM-676 (corundum) was used as a reference.

IR absorption spectra were obtained on a Bomem MB-102 FTIR spectrometer in the region 250—4000 cm^{-1}. Samples were prepared as suspensions in Nujol and pressed as KBr pellets.

Thermogravimetric analysis was performed with a Netzsch STA-449 system. Analysis was carried out in the temperature-programmed regime in Ar or hydrogen flow with a rate of 150 mL min^{-1}. The temperature was increased with a rate of 5—10 K min^{-1}. A catalyst sample (50—100 mg) was placed in platinum crucibles.

Catalytic studies of the hydrogenation of benzene to cyclohexane and the preferential hydrogenation of CO were carried out in fixed-bed flow reactors at atmospheric pressure. The reaction mixture contained C_6H_6—H_2 (12 : 88 (vol.%)) and CO—CO_2—H_2O—H_2 (1 :21 : 18 : 60 (vol.%)), respectively. In benzene hydrogenation, the flow rate of the mixture was 60 000 h^{-1}, while in CO hydrogenation it was varied from 3000 to 31 000 h^{-1}. Gas mixtures were analyzed by gas chromatography on a Kristall-2000 chromatograph. The benzene hydrogenation products were analyzed on a chromatographed equipped with two detectors (heat-conductivity and flame-ionization), whereas a heat-conductivity detector was used for the analysis of the products of CO hydrogenation. Columns packed with modified Chromosorb and active carbon SKT, respectively, were used for the separation of components of mixtures. The sensitivity threshold of chromatographic determination of the CO content was 10 ppm. The both reactions were carried out with a catalyst pellets 0.25—0.50 mm in size. Weighed samples of 0.25 and 0.16—0.76 g, respectively, were used. The catalytic properties in the hydrogenation reaction were characterized by the total conversion of benzene and the degree of its conversion into cyclohexane (selectivity), whereas in the preferential hydrogenation of CO to methane in the presence of CO_2 the catalytic properties were characterized by the residual content of CO and the selectivity for CO methanation, which was determined as the ratio of the CO consumption rate (W_{CO}) to the rate of methane formation (W_{CH4}). The catalytic studies were carried out on the samples precalcined in an inert gas at 400 °C (to prevent the oxidation of Cr^{3+} to Cr^{6+}) and then reduced in hydrogen at 300 °C.

Results and Discussion

Phase composition of the synthesized compounds and its changes upon the thermal treatment. The diffraction patterns of the precursor compounds are presented in Fig. 1. The diffraction patterns of the samples with the nickel content more than 60 at.% (NiCr-2.3/1 and NiCr-3/1) exhibit a set of broad diffraction lines in the range $2\theta \approx 10$—70°. The position of reflections and the distribution of their intensities correspond to the characteristics of nickel—chromium hydroxocarbonate (HOC) with the stichtite-type structure ($Mg_6Cr_2(OH)_{16}CO_3 \cdot 4H_2O$).[11,12] Stichtite is isostructural to minerals pyroaurite and hydrotalcite $M_6^{2+}M_2^{3+}(OH)_x(CO_3)_y \cdot nH_2O$ (M^{3+} = Fe^{3+} or Al^{3+}). These structures have a bilayer hexagonal packing of the anions $(OH)^-$, whose octahedral sites contain randomly distributed cations M^{2+} and M^{3+} (see Refs 13 and 14). The layers $[M^{II}_{1-x}M^{III}_x(OH)_2]^{x+}$ are linked by the carbonate anions and water molecules distributed between the layers. The structure of the compounds can contain nitrate anions along with carbonate anions. Figure 2 (curve *1*) shows the IR spectrum of HOC NiCr-2.3/1 exhibiting the absorption bands (AB) at 3423 and 1627 cm^{-1} assigned to vibrations of water molecules and the band at 1470 cm^{-1} attributed to vibrations of carbonate anions (CO_3^{2-}). Nitrate anions (NO_3^-) are present in the sample structure, and the band at 1384 cm^{-1} corresponds to these anions. The observed spectrum of HOC corresponds to a layer compound of the stichtite type.[15,16]

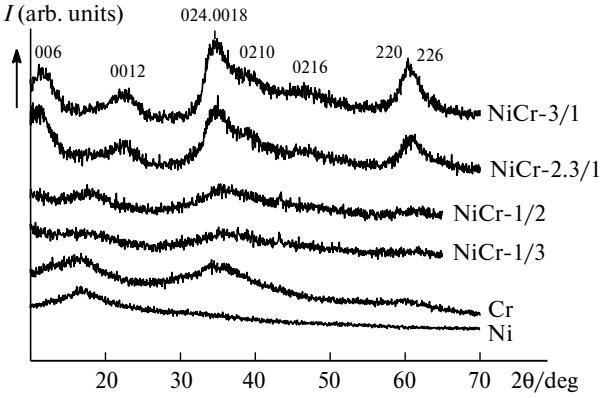

Fig. 1. Diffraction patterns of the studied Ni—Cr precursors differing in the relative atomic content of cations. The reflection indices (*hkl*) for the stichtite structure [ICDD-PDF2 00-045-1475] are indicated at the top.

The thermal treatment in an inert gas of the precursor compounds leads to the decomposition of HOC. The thermal analysis data for the sample NiCr-2.3/1 are presented in Fig. 3.

In addition to the endothermic effect of water removal at ~140—150 °C, two effects, namely, an endothermic peak with a maximum at 320 °C (loss 18.6 wt.%) and a weak exothermic peak with a maximum at ~500 °C (loss 2.2 wt.%) are observed in the curves. Figure 4 exhibits the diffraction patterns of the nickel—chromium samples obtained after thermal treatments at 400 and 600 °C. The positions of the strongest peaks due to phases NiO and $NiCr_2O_4$ (according to the tabulated data) are observed in the diffraction patterns. An analysis of the diffraction line positions suggests that the thermal treatment at 400 °C produces a phase with the structure of the NiO type with the unit cell parameter $a = 4.186 \pm 0.005$ Å somewhat increased compared to the tabulated data. The estimation of the particle size performed from the analysis of the diffraction line broading shows that a nanosized phase (3—4 nm) is formed. After the thermal treatment at 600 °C, the lattice parameter of this phase decreases to $a = 4.177$ Å

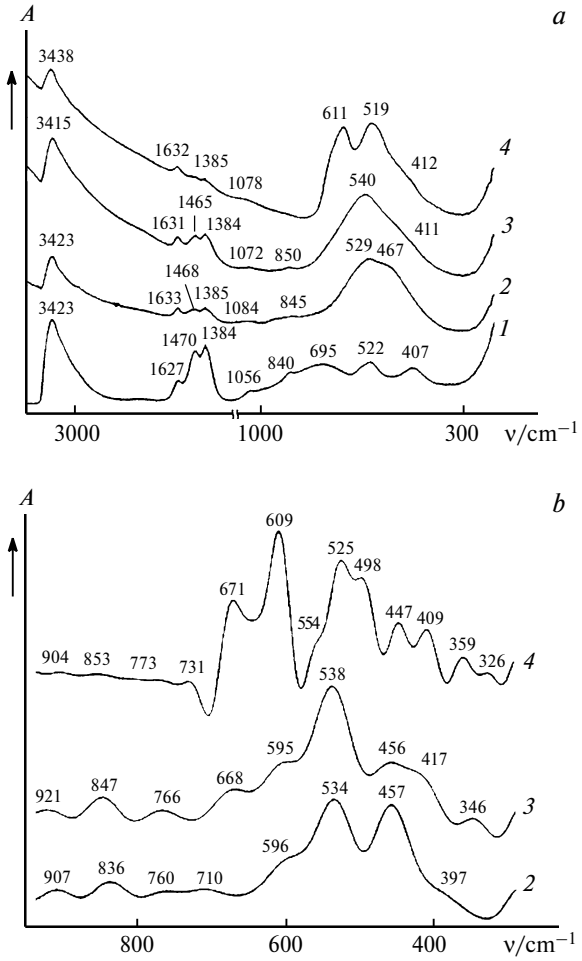

Fig. 2. Data of IR spectroscopy for the sample $Ni_{0.67}Cr_{0.33}$ (*a*) and its spectra at 250—900 cm^{-1} obtained by deconvolution (*b*): dry hydroxocarbonate (*1*), the sample calcined in argon at 400 °C before (*2*) and after its reduction in hydrogen at 300 °C (*3*), and the sample calcined in argon at 600 °C (*4*).

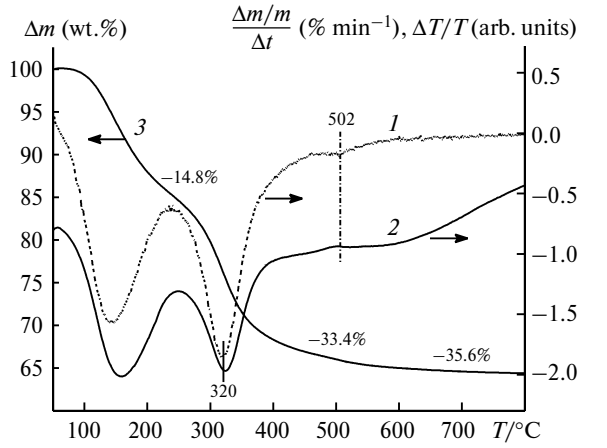

Fig. 3. Thermal curves DTG (*1*), DTA (*2*), and TG (*3*) of nickel—chromium hydroxocarbonate $Ni_{0.67}Cr_{0.33}$; argon flow rate 150 mL min^{-1}, 100 mg, and 10 °C min^{-1}.

corresponding to the tabulated value for NiO, and the phase of nickel chromite appears with the structure of cubic spinel with the parameter $a = 8.320 \pm 0.005$ Å, which coincides with the tabulated value.

According to the data of IR spectroscopy, the spectrum of HOC Ni—Cr calcined at 400 °C (see Fig. 2, curve *2*) exhibits a decrease in the AB intensity at 3423, 1627 cm^{-1} and 1470, 1384, 1056, 840 cm^{-1} related to the absorption of water and vibrations of the CO_3^{2-} and NO_3^- anions, respectively. It was found by deconvolution that the contour of the broad AB in the region 300—700 cm^{-1} contains the AB at 457 cm^{-1}, which is attributed to the absorption of NiO,[17] and the AB at 596, 397 cm^{-1} close to the AB to spinel[18] and the AB at 534 cm^{-1}, which can characterize the amorphous chromium compound with the same nearest surroundings as that in CrOOH.[19] After the sample was calcined at 600 °C (see Fig. 2, curve *4*), the AB at 611 (ν_1) and 519 cm^{-1} (ν_2) related to triply degenerate vibrations (F_{1u}) of the octahedral group of MO_6 become well discernible. The contours of the observed bands are broadened. Due to deconvolution one can see that each of them is split into two components: 671, 609 cm^{-1} and 525, 498 cm^{-1} ($A_{2u} + E_u$), and the AB at 359, 326 cm^{-1} ($A_{2u} + E_u$) can additionally be discriminated, which corresponds to vibrations of the octahedral and tetrahedral groups characteristic of the spectrum of nickel chromite spinel.[18,20] The splitting of the AB can be due to the presence of different cations (Ni^{2+}, Cr^{3+}) in the same crystallographic positions. The AB at 447 and 409 cm^{-1} in the IR spectrum of the sample are probably the result of splitting of the AB at 457 cm^{-1} assigned to the absorption of nickel oxide. Thus, the data of IR spectroscopy agree with and supplement the X-ray diffraction results.

Based on the data of X-ray diffraction analysis and IR spectroscopy, we may conclude that the synthesized HOC

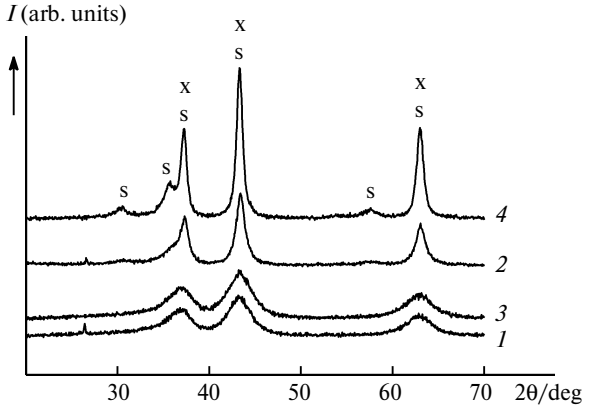

Fig. 4. Diffraction patterns of the nickel—chromium samples $Ni_{0.67}Cr_{0.33}$ (NiCr-2.3/1) (*1*, *2*) and $Ni_{0.73}Cr_{0.27}$ (NiCr-3/1) (*3*, *4*) calcined in argon at 400 °C (*1*, *3*) and 600 °C (*2*, *4*). The reflections of NiO (x) [ICDD, PDF-2, 00-047-1049] and (s) $NiCr_2O_4$ [ICDD, PDF-2, 00-023-1271] are marked.

containing more than 60 at.% nickel (NiCr-(2.3—3)/1) are single-phase systems with the stichtite-type structure. The thermal treatment of these precursors in an inert gas in the temperature range from 320 to 450 °C produces the combined nickel-chromium oxide with the structure of the NiO type modified by foreign anions. The removal of these anions at ~600 °C results in the formation of stoichiometric nickel oxide and nickel chromite with the spinel structure.

As follows from the X-ray diffraction data (see Fig. 1), the samples containing less than 40 at.% nickel (NiCr-1/3 and NiCr-1/2) are poorly crystallized. The diffraction patterns contain broad halos near $2\theta \approx 18$, 35, and 60°. A similar diffraction picture with halos in the vicinity of the same angles can be observed in the diffractograms of chromium and nickel HOC prepared as reference samples. The sample of nickel HOC shows the halo near $2\theta \approx 18°$ (see Fig. 1). The positions of reflections of the chromium and nickel HOC agree with the angles of the strongest reflections found among the reference data. For the studied samples NiCr-1/3 and NiCr-1/2, the formation of combined nickel—chromium HOC can be suggested because the samples were prepared by the method of combined coprecipitation of nickel and chromium. It appears that the presence of some amount of a particular phase of the chromium HOC cannot be excluded, since the samples contain chromium in an excessive amount. No compound with the stichtite structure is observed.

The X-ray diffraction data are in agreement with the results obtained from IR spectra. Figure 5 show the IR spectra of the nickel—chromium HOC NiCr-1/3 and NiCr-1/2, the spectra of chromium (Cr) and nickel (N) HOC, and the spectrum of the sample containing more than 60 at.% nickel (NiCr-3/1). It can be seen that the spectra of the low-nickel samples in the region 300—700 cm^{-1} are actually different from the spectrum of the sample with the stichtite structure. The spectra of the samples NiCr-1/3 and NiCr-1/2 show weak AB at 695 and 407 cm^{-1} and a strong AB at 522 cm^{-1}. A similar ratio of AB intensities in the considered region can be observed in the spectrum of the chromium HOC sample as well.

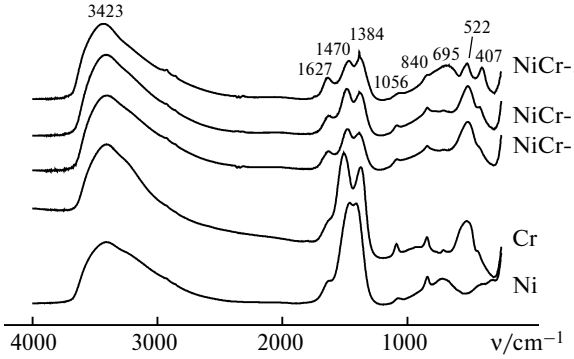

Fig. 5. IR spectra of the nickel—chromium hydrocarbonate samples with different relative atomic contents of cations.

The results of thermal analysis of the sample with a low nickel content are shown in Fig. 6. The thermal curves exhibit the effect of water removal at ~130—140 °C and also three effects: (1) an endothermic peak with a maximum at ~355 °C accompanied by the loss of 12.5 wt.%; (2) a weak exothermic peak with a maximum at ~540 °C; and (3) an exothermic peak with a maximum at ~640 °C. The effects in the region ~540—640 °C are accompanied by a total weight loss of ~4.4%.

The results of X-ray diffraction analysis of the NiCr-1/2 sample calcined at 400 and 650 °C are presented in Fig. 7. Three halos, which could be attributed to the cubic structure of the NiO type with an increased unit cell parameter are observed in the diffraction patterns of the samples treated in argon at 400 °C, but the line with $d^{max}_{311} \approx$ ≈ 2.4—2.5 Å is the most intense in the spectrum of the sample, which is not characteristic of the structure of the NiO type. The synthesized compound corresponds, to a greater extent, to highly dispersed spinel. The structure of this compound represents a three-layer cubic closest packing with disorder of nickel and chromium cations, being "protospinel" according to the literature data.[21] The treatment at 650 °C, causes ordering among cation distribution and the formation of the structure of cubic spinel $NiCr_2O_4$ with the unit cell parameters $a = 8.320 \pm 0.005$ Å. The diffraction pattern (Fig. 7) also shows weak reflections, indicating the presence of traces of the Cr_2O_3 phase, which confirms the assumption about some inhomogeneity of the precursor compounds of samples of this composition: nickel—chromium HOC NiCr-1/(2—3). According to the X-ray diffraction result, the thermal effect at ~355 °C is related to the decomposition of nickel and chromium HOC, the removal of CO_2 and H_2O, and the formation of the disordered nanodispersed structure of nickel—chromium spinel. The effects in the region ~540—650 °C characterize the processes of formation and

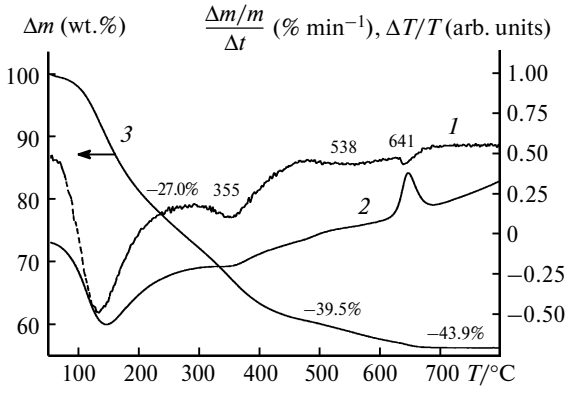

Fig. 6. Thermal curves DTG (*1*), DTA (*2*), and TG (*3*) of nickel—chromium hydroxocarbonate $Ni_{0.33}Cr_{0.67}$ (NiCr-1/2); argon flow rate 150 mL min^{-1}, 50 mg, and 10 °C min^{-1}.

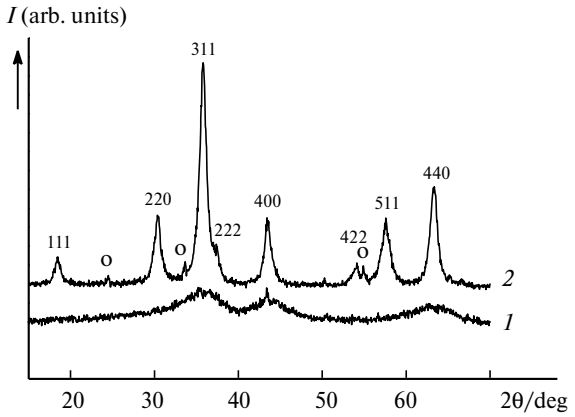

Fig. 7. Diffraction patterns of the sample $Ni_{0.33}Cr_{0.67}$ calcined at 400 (*1*) and 650 °C (*2*) in an argon flow. Figures at the top are reflections of the phase $NiCr_2O_4$; the reflection of Cr_2O_3 traces is marked (o).

crystallization of the structure of cubic spinel $NiCr_2O_4$ (and Cr_2O_3).

Thus, the study of the structural characteristics of the synthesized precursors of the nickel—chromium samples with high and low nickel contents shows that HOC with the nickel content more than 60 at.%, NiCr-(2.3—3)/1, represent homogeneous systems with the stichtite structure. At the same time, the samples with the nickel content less than 40 at.%, NiCr-1/(2—3), consist mainly of combined HOC of nickel and chromium. The calcination of the precursors of the nickel—chromium catalysts with high and low nickel contents in an inert gas at medium temperatures (300—400 °C), which is often used in thermal treatments of catalysts, results in the formation of oxide compounds of different structures. A combined oxide with the structure of the NiO type modified by admixture anions is formed from HOC $Ni_{0.67—0.73}Cr_{0.33—0.27}$, while nickel—chromium spinel with the disordered structure is formed from HOC $Ni_{0.23—0.33}Cr_{0.77—0.67}$.

Reductive activation of nickel—chromium HOC precalcined in argon at 400 °C was carried out in a hydrogen environment at 300 °C for 2 h.

According to the X-ray diffraction data, the activation of the high-nickel samples, NiCr-(2.3—3)/1, results in the formation of a phase of nickel metal with the Ni^0 particle size ~5.5 nm. The presence of reflections of the oxide phase of the precursor indicates the incomplete reduction of the Ni^{2+} cations in the catalyst. The IR spectrum obtained by deconvolution of the reduced sample (see Fig. 2, curve *3*) contains AB, which are also observed in the spectrum of the sample calcined in argon at 400 °C. However, the intensity of the AB at 457 cm^{-1} (Ni—O) decreases, which may indicate the reduction of nickel cations from the nickel oxide phase.

In the low-nickel samples, NiCr-1/(2—3), the formation of Ni^0 is only indirectly indicated by the diffraction pattern, namely, by an increased line intensity in the region of $d \approx 2.09$—2.03 Å.

The surface area of metallic nickel particles formed on the catalyst surface due to hydrogen activation was determined by the method of hydrogen chemisorption on the surface of the reduced catalysts. The coverage of the nickel surface with hydrogen atoms was accepted to be 1, $\theta_H = 1$. It was found that the samples NiCr-2.3/1 and NiCr-3/1 have similar values of the specific surface of Ni^0 (7.0 ± 0.5 m^2 g^{-1}) and the surfaces of the samples NiCr-1/3 and NiCr-1/2 are similar, being more than two times lower: 3.0 ± 0.5 m^2 g^{-1}.

Catalytic characteristics of the samples in the reaction of benzene hydrogenation are presented in Table 1. It was accepted for the determination of the hydrogenation rate constant that this reaction has the first order with respect to benzene.

The data in Table 1 show that the rate constants for cyclohexane formation expressed per 1 m^2 of the metal Ni surface vary by a factor of ~4 for the samples with the high and low nickel content. The conversion of benzene is substantially higher on the sample NiCr-2.3/1, whose precursor compound has the stichtite-type structure and after calcination represents a combined oxide of nickel and chromium cations with the structure of the NiO type modified by admixture anions. Cyclohexene is formed in a comparable amount as a by-product on the both catalysts.

In the reaction of CO hydrogenation with excess CO_2, only the catalyst NiCr-2.3/1 was studied. As follows from Fig. 8, at a gas flow rate of 7000 h^{-1} the depth of purification from CO up to 10 ppm in the temperature range 175—200 °C was achieved with the catalyst. In this case, the selectivity of methanation for CO varies from ~1 to ~0.5. At 175 °C methane is formed almost only from CO; with the temperature increase to 200 °C methane is formed from CO and CO_2 in equal amounts, *i.e.*, during hydrogenation 1 mole of CO is hydrogenated by 1 mole of CO_2 (the conversion of CO approaches 100% and the conversion of CO_2 is ~4.8%). When the temperature increases to

Table 1. Catalytic properties of the samples in the hydrogenation of benzene[a]

Catalyst	$S^{\circ}_{sp(Ni)}$ /m^2 g^{-1}	T /°C	k /s^{-1} m^{-2}	C^b	S^c
				%	
NiCr-2.3/1	7.0	120	2.8	85	93
		140	6.2	88	94
NiCr-1/2	3.0	120	0.7	14	87
		140	1.6	18	90

[a] Reaction mixture C_6H_6—H_2 (12 : 88 vol.%), contact time 0.06 s.

[b] Conversion of benzene.

[c] Selectivity of cyclohexane formation.

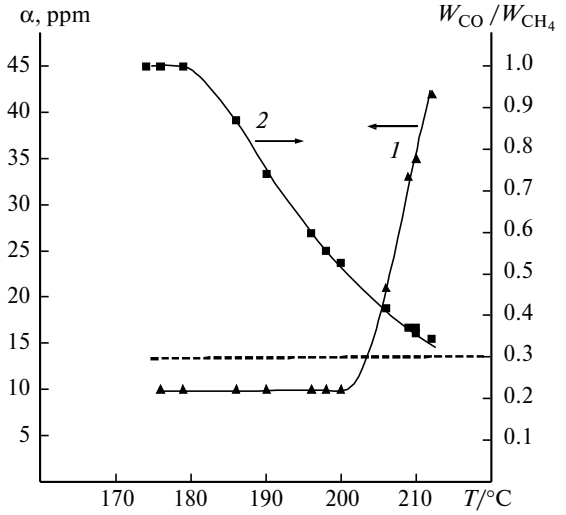

Fig. 8. Changes in the volume fraction (α) of CO (*1*) and the selectivity of CO methanation (W_{CO}/W_{CH_4}) (*2*) at different reaction temperatures on the catalyst NiCr-2.3/1 at a flow rate of the reaction mixture of 7000 h^{-1}. Reaction mixture $CO—CO_2—H_2O—H_2$ (1 : 21 : 18 : 60) (vol.%). Dashed line designated the required level of selectivity.

205 °C, the residual concentration of CO increases to 20 ppm and the selectivity of methanation for CO decreases to 0.43. An increase in the reaction gas consumption results in a decrease in the depth of gas purification from CO and in the preferential character of CO hydrogenation.

Thus, the reaction of benzene hydrogenation on the oxide nickel—chromium catalysts is sensitive to the composition and structure of the precursor compound Ni—Cr HOC, and the latter are determined to a considerable extent by the Ni^{2+}/Cr^{3+} ratio in the catalyst. At high nickel contents (Ni^{2+}/Cr^{3+} = (2.3—3)/1) HOC with the structure of the mineral stichtite type are formed; their thermal treatment and subsequent reduction provide the formation of highly active and selective crystallites of metal nickel. The nickel—chromium oxide catalyst synthesized from the precursor compound of the stichtite type is also highly active and selective for the reaction of preferential hydrogenation of CO in the presence of CO_2.

At low nickel contents, Ni^{2+}/Cr^{3+} = 1/(2—3), no similar structure is formed and the catalysts manifest no high activity.

The authors are grateful to E. V. Sopova for DTA analysis.

References

1. S. Takenaka, T. Shimizu, K. Otsuka, *Inter. J. of Hydrogen Energy*, 2004, **29**, 1065.
2. M. B. I. Choudhury, S. A. Mazen, A. S. Tomoyuki, *Appl. Catal., A*, 2006, **314**, 47.
3. F. Cárdenas-Lizana, S. Gómez-Quero, M. A. Keane, *Appl. Catal., A*, 2008, **334**, 119.
4. A. C. A. Monteiro-Gezork, R. Natividad, J. M. Winterbottom, *Catal. Today*, 2008, **130**, 471.
5. P. G. Savva, K. Goundani, J. Vakros, K. Bourikas, Ch. Fountzoula, D. Vattis, A. Lycourghiotis, Ch. Kordulis, *Appl.Cat., B*, 2008, **79**, 199.
6. J. H. Bitter, M. K. Lee, A. G. T. Slotboom, A. J. Dileen, K. P. Jong, *Catal. Lett.*, 2003, **89**, 139.
7. L. Daza, B. Pawelec, J. A. Anderson, J. L. G. Fierro, *Appl.Cat.*, 1992, **87**, 145.
8. G. A. Martin, J. A. Dalmon, *J. Catal.*, 1982, **75**, 233.
9. R. Molina, G. Poncelet, *J. Catal.*, 2001, **199**, 162.
10. M. Boudart, C. M. M. Conica, *J. Catal.*, 1989, **117**, 33.
11. H. F. W. Teilor, *Mineralog. Mag.*, 1973, **39**, 377.
12. S. K. Mondal, T. K. Baidya, *Mineralog. Mag.*, 1996, **60**, 836.
13. A. S. Bookin, V. I. Cherkashin, V. A. Drits, *Clays Clay Minerals*, 1993, **41**, 558.
14. E. K. Vasiliev, N. P. Vasilieva, *Rentgenograficheskii opredelitel´ karbonatov* [*The X-ray Diffraction Identifier of Carbonates*], Nauka, Novosibirsk, 1980, 143 (in Russian).
15. M. J. Hernandez-Moreno, M. A. Ulibarri, J. L. Rendon, C. J. Serna, *Phys. Chem. Minerals*, 1985, **12**, 38.
16. R. L. Frost, K. L. Erickson, *Spectrochimica Acta, Part A-Mol. Biomol. Spectr.*, 2004, **60**, 3001.
17. E. N. Yurchenko, G. N. Kustova, S. S. Batsanov, *Kolebatel´nye spektry neorganicheskikh soedinenii* [*Vibrational Spectra of Inorganic Compounds*], Nauka, Novosibirsk, 1981, 91 (in Russian).
18. J. Preudhomme, P. Tarte, *Spectrochimica Acta*, 1971, **27A**, 1817.
19. P. L. A. Ratnasamy, *J. Phys. Chem.*, 1972, **76**, 1839.
20. S. Hafner, *Z. Kristallogr.*, 1961, **119**, 331.
21. B. G. Erenburg, V. P. Fateeva, L. I. Likhovid, A. I. Min´kov, *Izv. Sib. Otd. Akad. Nauk SSSR* [*Bulletin of Siberian Branch of Academy of Sciences of the USSR*], 1981, **2**, 51 (in Russian).

Received August 31, 2010;
in revised form October 11, 2010